tvst

Article

Longitudinal Testing of Retinal Blood Flow in a Mouse Model of Hypertension by Laser Speckle Flowgraphy

Michelle R. Tamplin[1,2], Kimberly A. Broadhurst[1], Anthony H. Vitale[1], Ryuya Hashimoto[2], Randy H. Kardon[2,3], and Isabella M. Grumbach[1–3]

[1] Department of Internal Medicine, Carver College of Medicine, University of Iowa, Iowa City, IA, USA
[2] Department of Ophthalmology and Visual Sciences, Carver College of Medicine, University of Iowa, Iowa City, IA, USA
[3] Iowa City Veterans Affairs Healthcare System, Iowa City, IA, USA

Correspondence: Isabella M. Grumbach, Division of Cardiovascular Medicine, Department of Internal Medicine, University of Iowa, 169 Newton Road, 4336 PBDB, Iowa City, IA 52242, USA. e-mail: isabella-grumbach@uiowa.edu
Randy H. Kardon, Department of Ophthalmology and Visual Sciences, University of Iowa, 200 Hawkins Drive (PFP), Iowa City, IA 52242, USA. e-mail: randy-kardon@uiowa.edu

Received: November 2, 2020
Accepted: January 15, 2021
Published: February 12, 2021

Keywords: laser speckle flowgraphy (LSFG); hypertension; retinal blood flow; retinal vasculature

Citation: Tamplin MR, Broadhurst KA, Vitale AH, Hashimoto R, Kardon RH, Grumbach IM. Longitudinal testing of retinal blood flow in a mouse model of hypertension by laser speckle flowgraphy. Trans Vis Sci Tech. 2021;10(2):16, https://doi.org/10.1167/tvst.10.2.16

Purpose: The purpose of this study was to investigate the applicability of laser speckle flowgraphy (LSFG) for a longitudinal study of blood flow parameters in mice before, during, and after continuous infusion of angiotensin-II.

Methods: Normotensive C57BL/6J mice were imaged by LSFG at one ($n = 22$) or three sessions ($n = 10$). Two additional cohorts were imaged by LSFG before, during, and after continuous infusion of angiotensin-II by minipump for 2 or 4 weeks ($n = 6$ and 8, respectively). Retinal blood flow, vascular resistance, and total area of retinal vascular flow, a surrogate of vascular remodeling and vasoconstriction, were determined at each time point.

Results: During infusion of angiotensin-II for 2 weeks, decreased retinal blood flow and area of vascular flow, as well as increased vascular resistance, were observed. These changes were reversed 1 week after the end of angiotensin-II infusion. In mice infused with angiotensin-II for 4 weeks, decreased retinal blood flow and increased vascular resistance persisted at 6 weeks postinfusion, despite a decrease in blood pressure.

Conclusions: Arterial hypertension, induced by continuous angiotensin-II infusion, results in reduced retinal blood flow, increased vascular resistance, and decrease in area of intravascular blood flow within retinal arterioles and venules. Sustained vasoconstriction 6 weeks after the end of a 4-week period of angiotensin-II infusion may indicate vascular remodeling after a period of chronic hypertension.

Translational Relevance: Retinal LSFG is useful for serial investigation of blood flow in mouse models and provides a novel approach for translational studies on the microvascular effects of hypertension in vivo.

Introduction

Current modalities to image the ocular vasculature provide complementary tools to assess the different aspects of ocular microvascular structure and function. Although indocyanine green angiography is particularly effective for visualizing choroidal microvessels, it provides only limited information on blood flow.[1] Doppler optical coherence tomography (OCT) has been used for noninvasive, high-resolution imaging of the retinal and choroidal vasculature.[2] However, this technology requires significant adaptation and postprocessing to measure absolute blood flow velocity.[3] Currently, it is not commercially available or US Food and Drug Administration (FDA)-approved for use with human subjects. Conversely, ocular laser speckle flowgraphy (LSFG) has been deployed to investigate retinal and choroidal blood flow in humans, while lacking the high resolution to depict capillaries

of doppler OCT. LSFG is based on the changes in the speckle pattern of laser light reflected from the fundus of the eye. The mean blur rate (MBR), derived from the contrast of the speckle pattern, is linearly proportional to blood flow velocity[4] and microsphere-derived volume blood flow[5] over the range observed in human and animal retinal vessels. With its measurement by LSFG, ocular blood flow has been studied under physiologic conditions[6–8] and in various ophthalmic diseases, such as glaucoma and ischemic optic neuropathy.[9–11] Additional studies have also reported on its application to study systemic cardiovascular physiology, for example, in patients undergoing cardiac surgery, during normal pregnancy,[7] and with gestational hypertension, as well as in patients with sleep apnea and metabolic syndrome.[12–16]

The recent development of LSFG instrumentation for small animals provides an opportunity to perform parallel studies of retinal blood flow in human patients and relevant animal models of disease. This approach could facilitate both bench-to-bedside research and reverse translation. Although a detailed, quantitative analysis of blood flow changes over a period of several months in rats is feasible,[17] the reports on LSFG in mice have been very limited so far to single measurements in genetically modified strains.[18,19] Thus, it remains to be established whether a more detailed analysis of blood flow parameters is feasible and whether repeat measurements can reliably detect acute and chronic changes, for example, by vasoactive substances. In this study, we compare analysis approaches to quantitate retinal blood flow in C57BL/6J mice and perform longitudinal measurements in mice with infusion of angiotensin-II (Ang-II) to assess retinal blood flow, vascular resistance, vasoconstriction, and potential vascular remodeling.

Methods

Study Cohorts

All experimental procedures were approved by the University of Iowa and the Iowa City VA Health Care System Institutional Animal Care and Use Committees. All procedures were in compliance with the standards for the care and use of laboratory animals of the Institute of Laboratory Animal Resource, National Academy of Science. Male C57BL/6J mice were purchased from Jackson Laboratories (strain #000664). Experiments were performed on mice between 10 and 12 weeks of age. Mice were housed in a room with controlled temperature (23°C) and a dark/light cycle of 12 hours. All mice had free access to water and standard rodent chow. All measurements were performed between 9 AM and 12 AM to avoid circadian variations.

Four cohorts of male black C57BL/6J mice were studied. (1) Baseline cohort: 22 mice were imaged at one session. (2) Baseline cohort for repeat measurements: 10 mice were imaged over 3 sessions to determine intersession variability. (3) Short-term cohort: 6 mice were infused with Ang-II for 2 weeks. Measurements were performed before, during, and 1 week after the end of Ang-II infusion. (4) Long-term cohort: 8 mice were infused with Ang-II for 4 weeks. Imaging was performed before, during, and 6 weeks after the end of Ang-II infusion.

Ang-II Infusion by Osmotic Mini-Pumps

Osmotic mini-pumps (Alzet Osmotic Pumps, model 1002 or 2004, respectively; DURECT) were filled with sterile phosphate-buffered saline (PBS) or Ang-II (0.625 μg/kg/min). Briefly, mice were anesthetized with an intraperitoneal (IP) injection (0.1 mL/20 g body weight) of ketamine/xylazine solution (VetaKet/AnaSed,17.5 mg/mL; 2.5 mg/mL). Pumps were implanted subcutaneously along the right flank through a subscapular incision, which was then closed using absorbable sutures (Ethicon). Pain control was provided by subcutaneous (SC) injections (0.1 mL/20 g body weight) of meloxicam (Loxicom; Norbrook Laboratories, 0.2 mg/mL,) for 2 days postoperatively. Any remaining sutures were removed on day 10.

Tail Cuff Blood Pressure Measurements

Blood pressure was monitored daily by the tail cuff method (Visitech Systems) after a 5-day training period before the minipumps were implanted. The mice were placed in the holders on a heated platform (37°C) and then given 5 minutes to warm up and settle down. After 5 initial blood pressure (BP) measurements, 20 additional measurements were taken over 20 minutes. The data from 3 consecutive days were averaged. Mice were retrained 2 days before repeat BP measurements.

Laser Speckle Flowgraphy

Blood flow measurements were obtained in mice anesthetized by IP injection of 17.5 mg/mL ketamine/2.5 mg/mL xylazine solution (VetaKet/AnaSed, 0.1 mL/20 g body weight). Mice were placed on an infrared heating pad controlled by a rectal temperature probe (PhysioSuite; Kent Scientific) and the body core temperature was maintained at

37°C. For some measurements in cohort 1, the core temperature of the mouse was raised gradually to 39°C. Five successive measurements of intraocular pressure (IOP) were taken in the right eye using a handheld tonometer (Tonolab TV02; Icare). BP was recorded in anesthetized mice during the imaging procedure using an automatic tail-cuff plethysmography system (CODA Monitor; Kent Scientific). The measurements were used to determine the ocular perfusion pressure (OPP), which was calculated as follows: OPP = (mean arterial pressure − IOP),[20] where mean arterial pressure = diastolic BP + ⅓ (systolic BP − diastolic BP).

Blood flow measurements were obtained using LSFG-Micro (Softcare Co., Ltd.), which uses a charge-coupled device (700 × 480 px) camera attached to a diode laser (830 nm wavelength) and microscope (SZ61TR; Olympus Corporation) to detect interference patterns produced when the light reflecting back from cells passes through the field of the laser. The instrument setup is depicted in Supplementary Figure S1. Images are acquired continuously over 4 seconds at a rate of 30 frames per second to produce a temporal composite of a 3.2 × 2.5 mm^2 area. The blur of the speckle pattern produced by the detected interference is quantified as the MBR, a relative index of blood flow velocity expressed in arbitrary units (AUs).

LSFG Analysis for Determination of Retinal Blood Flow

To analyze blood flow, composite images of blood flow averaged at each pixel over the 4 second recording period (Fig. 1A) were opened in the LSFG Analyzer software (version 3.5.0.0; Softcare, Co., Ltd.). Two alternative methods were used to quantify retinal blood flow: (1) measurement of total retinal blood flow within retinal arterioles and venules located within a large user-defined annular area of retina outside of the optic nerve head, and (2) summated blood flow measured within individual retinal arterioles and venules. Unlike the retina of larger species, it is not possible to reliably differentiate arterioles from venules with the software tools currently available to quantify laser speckle blood flow, so flow summated in both vessels is reported.

In the first, annulus defined method, the first circle (termed a "rubber band" or "RB" by the Analyzer) was centered on the optic nerve head and drawn to totally encompass the structure (see Fig. 1B). The second circle was positioned starting at the margin of the first circle and extended circumferentially to include the retinal vessels in a large annulus of the mouse retina (see Fig. 1B). Blood flow was measured in the annular area defined by the second circle, excluding the optic nerve head. Blood flow signal from the choroidal vascular bed was not attainable due to signal attenuation from absorption of the 830 nm light by the heavily pigmented fundus of the black C57BL/6J mouse strain. Any signal measured outside of the intravascular flow of retinal arterioles and venules is classified as extravascular tissue flow, termed "MT" by the Analyzer software (darkest blue color in Figs. 1A, 1B, black area in Fig. 1D). The cutoff level for extravascular tissue flow is automatically calculated by the Softcare analysis software, which defines the threshold using the flow histogram of the composite image (see Fig. 1A). Flow signal above this threshold corresponds to flow in the retinal arterioles and venules ("MV," white signal in Fig. 1D).

In the second method, in which blood flow within individual vessels is measured, the Total Retinal Arteriole and Venule Analysis (TRAVA) alternative Softcare analysis software method was used. By this method, the user defines the vessel midline (yellow lines in Fig. 1C) and extends a rectangular box along a length of each measured retinal vessel that includes the lumen and a small retinal area outside of the lumen, considered background flow. The TRAVA software subtracts the background blur rate from the intraluminal blur rate to estimate the true intraluminal flow, devoid of any small blur signal underlying the retinal vessel in the same z-axis. The integral of flow in the resultant intraluminal area takes into consideration flow velocity and intraluminal dimension to yield retinal flow volume (RFV) of each defined vessel. The value TRFI/W (see Fig. 1C) is the result of correcting the RFV value for vessel width, and is used here to represent blood flow in individual vessels.

To measure overall changes in vessel width and hence total area of intravascular flow detected above an arbitrary flow level, a manual threshold was set at a mean blur rate equal to 7 (indicated in Fig. 2D). The "percent vessel area" measures the number of "white" pixels (or samples) above the threshold. By using a fixed threshold and keeping a fixed total sample pixel area by applying the same annulus to each image, a decrease in percent vessel area indicates decreased vessel luminal width caused by vasoconstriction and/or vascular remodeling (see Fig. 2D).

After placing the bands and selecting a thresholding method, scans were processed using the device's accompanying batch processing software, Cobitos (version 1.0.52.0; Softcare, Co., Ltd.). Ocular perfusion pressure, vascular flow, vascular resistance (ocular perfusion pressure divided by flow), percent vessel area, and other measures of blood flow were tabulated

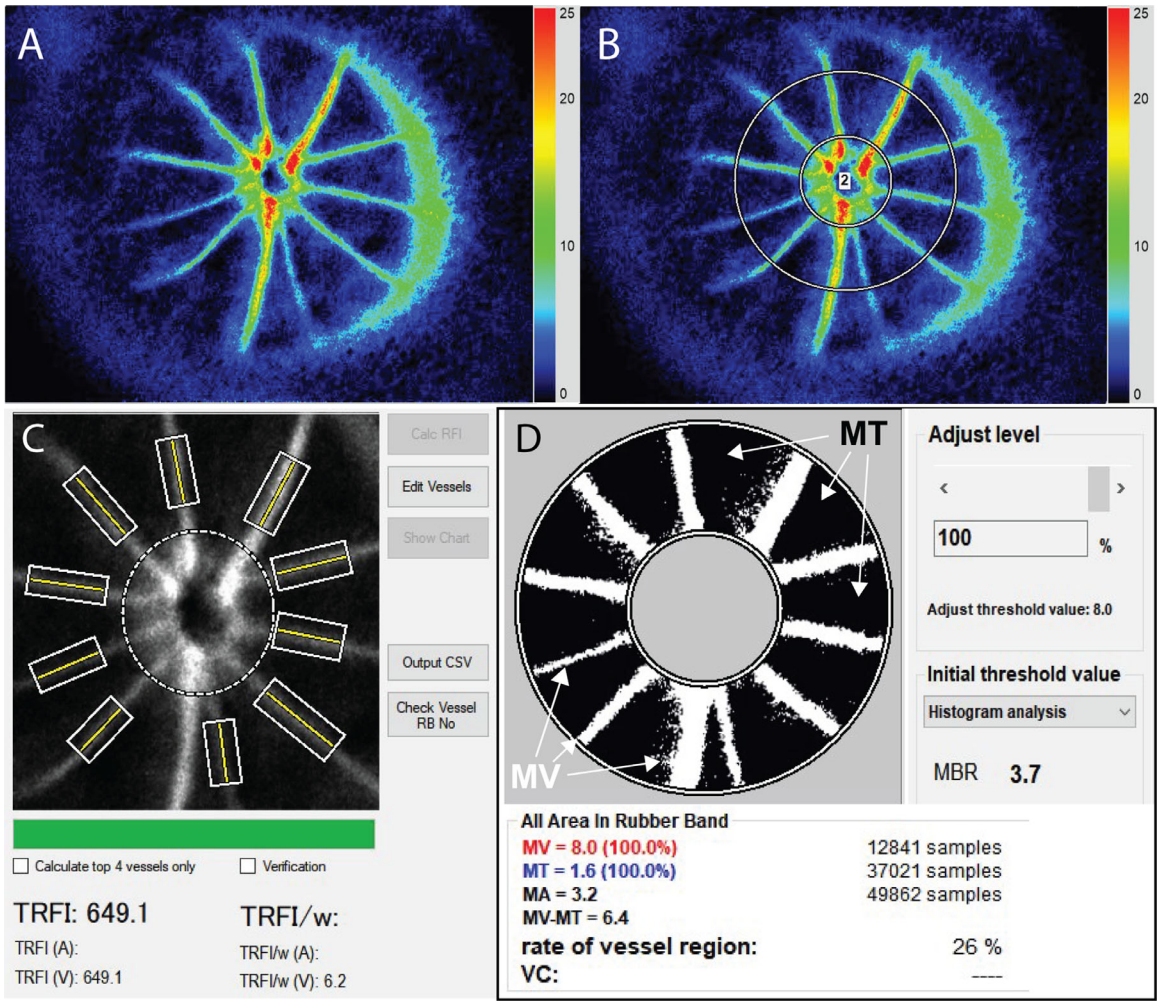

Figure 1. Analysis of LSFG images based on individual blood vessels (TRAVA method) and retinal annular method. (**A**) Representative LSFG composite image of the mouse retina, centered on the optic nerve head. The color scale represents the highest mean blur rate as *red* and the lowest as *blue*. The crescent at the right side of the image is an optical artifact. (**B**) Placement of circular regions of interest (ROI; *solid lines*) for analysis of retinal vessels outside of the optic nerve head. (**C**) In the Total Retinal Arteriole and Venule Analysis (TRAVA) method, individual blood vessels (*yellow*) are labeled for calculation of the width-corrected total retinal flow index (TRFI/W). (**D**) In the annulus method, an ROI is analyzed after selection of a threshold value by either automated histogram analysis or manual thresholding at MBR = 7. Signal above the threshold is counted as vascular blood flow (MV, white signal); below this threshold, surrounding extravascular tissue (MT, black signal).

for all scans in a spreadsheet exported to Microsoft Excel.

Statistical Analysis

Statistical analyses were performed using GraphPad Prism (version 8.0.0; GraphPad Software). The coefficient of variability was defined as 100% × (standard deviation)/(mean); for intersession variability, the standard deviation and mean across all 5 sessions were used. Interoperator statistics were calculated using the intraclass correlation coefficient.[21] Repeated measures 1-way ANOVA with Tukey's multiple comparison tests were performed unless indicated otherwise.

Results

Comparison of Blood Flow Analysis Utilizing Annulus Versus Individual Vessel Analysis

First, we performed LSFG scans in 22 control mice, to compare a selected vessel-based and a regions of interest (ROI)-based analysis. There was good agreement between the two methods ($r^2 = 0.615$, $P < 0.0001$; Fig. 3). Of note, because we were unable to distinguish arterioles from venules by scanning laser ophthalmoscope or color fundus images in the mouse optic nerve head, all vessels (arterioles and venules) were analyzed as one vessel category. The coefficient of

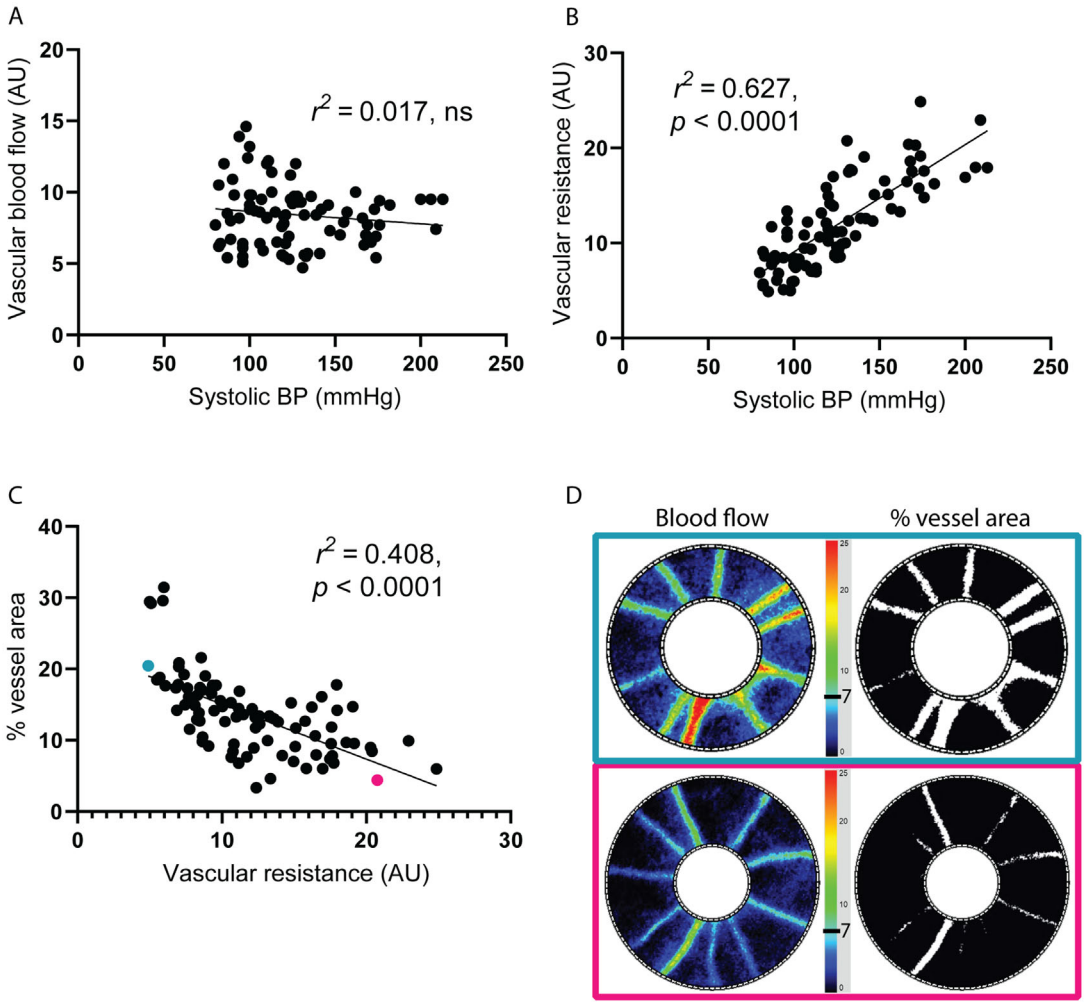

Figure 2. Regulation of retinal blood flow as a function of systolic blood pressure. (**A**) Vascular blood flow (MV) shown as a function of systolic blood pressure (SBP). (**B**) Vascular resistance (VR) as a function of SBP, with resistance calculated as the ocular perfusion pressure divided by the flow rate MV in **A**. (**C**) Percent vessel area in an annulus as a function of vascular resistance. Percent vessel area was calculated using a fixed threshold at MBR = 7, and was used to assess vessel luminal width. (**D**) Illustration of blood flow and percent vessel calculation in the case of lower (*teal*, as in **C**) and higher (*pink*, as in **C**) vascular resistance.

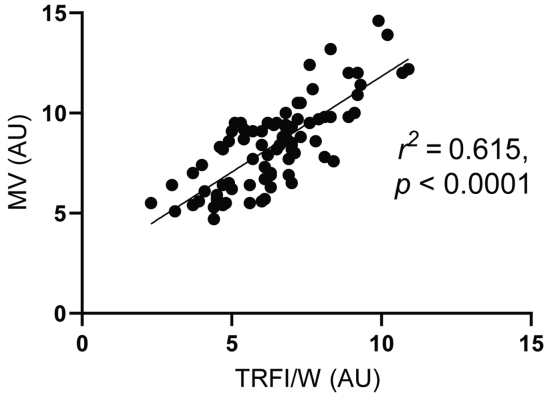

Figure 3. Linear regression analysis comparing blood flow between the annulus versus the TRAVA analysis methods. Linear regression comparison of the annulus versus TRAVA methods confirms viability of either method to detect blood flow, whether individual vessel boundaries are drawn (TRAVA) or average signal over an annulus is used.

variability for short-term repeat measurement variability between multiple scans taken at one session was lower for the annulus method compared to the TRAVA method (11.00% vs. 16.29%; Table). When three operators independently performed both analyses, interobserver variability by the intraclass correlation coefficient (ICC) was 0.928 for the annulus method vs. 0.687 for TRAVA (Supplementary Table S1). Next, we established intersession variability by performing LSFG scans in 10 mice over 3 weekly sessions. The mean intersession variability for the annulus method was similar to the TRAVA method (15.51% vs. 16.41%; Supplementary Table S2). Together, these findings suggest that overall, the annulus method provides measurements with the lowest intra- and inter-session variability; thus, the annulus method was used for analysis of the subsequent experiments.

Table. Comparison of Blood Flow Measure and Variability by Selected Blood Vessel (TRAVA, TRFI/W) and Annulus-Based (MV) Methods Over 4 Scans in 22 Control Mice

Control Mouse #	Mean TRFI/W (AU)	Mean MV (AU)	COV %, TRFI/W	COV %, MV
1	6.50	8.05	22.15	20.90
2	3.13	5.78	23.71	10.13
3	5.50	6.75	22.42	14.34
4	7.33	7.63	16.70	22.29
5	6.10	9.30	17.04	7.70
6	6.15	7.60	1.15	5.58
7	5.78	8.88	18.62	5.77
8	5.23	8.98	19.60	11.70
9	6.95	9.53	5.45	2.16
10	5.90	8.38	27.40	11.22
11	5.53	10.43	14.13	13.39
12	5.35	8.70	11.67	3.38
13	7.20	9.15	20.51	3.22
14	5.58	5.70	9.53	8.47
15	7.43	9.30	12.21	14.07
16	4.50	10.18	10.10	17.64
17	8.05	11.05	14.43	15.10
18	7.65	13.53	13.69	6.97
19	9.68	7.50	14.87	22.12
20	9.00	7.20	13.91	8.41
21	5.95	5.38	26.56	8.51
22	7.08	6.18	22.45	9.00
Mean	6.43	8.41	16.29	11.00
SD	1.47	1.94	6.62	5.94

Next, we determined the relationship between retinal blood flow and BP. Mild hyperthermia was used to induce BP increases. Vascular blood flow (MV) remained stable across a range of BPs, during single (see Fig. 2A) and across multiple sessions (Supplementary Figure S2). Thus, vascular resistance increased significantly with increasing BP ($P < 0.0001$; see Fig. 2B), signifying autoregulation. The percent vessel area, a surrogate measure of vessel width, decreased significantly with increasing vascular resistance and increasing BP ($P < 0.0001$; Figs. 2C, 2D).

Alterations in Blood Flow Dynamics With Ang-II-Induced Hypertension

Next, hypertension was induced in mice by continuous infusion of Ang-II over 2 weeks (Fig. 4A). The systolic BP by tail cuff measurements rose from an average of 123 mm Hg at baseline to 149 mm Hg on day 14 (Fig. 4B). The systolic BP was at similar levels during the LSFG measurement (116 mm Hg at baseline, and 156 mm Hg on day 14 of Ang-II infusion; Fig. 4C). BP returned to baseline levels within 7 days after cessation of Ang-II infusion (102 mm Hg on day 21; see Fig. 4C). Ocular perfusion pressure, taking into account IOP, varied in the same manner (Fig. 4D). Vascular blood flow decreased with increasing BP and ocular perfusion pressure (8.7 AU at baseline, and 7.7 AU on day 14); it returned to baseline levels by day 21 (9.5 AU; Fig. 4E). Accordingly, vascular resistance increased significantly with Ang-II infusion (10.1 AU at baseline, and 15.7 AU on day 14, $P < 0.01$) and returned to baseline levels by day 21 (8.0 AU; Fig. 4F). The percent vessel area declined with increasing vascular resistance and decreasing blood flow (11.3% at baseline, and 8.8% on day 14); by day 21, it returned to baseline levels (13.0%, $P < 0.01$; Fig. 4G).

Decreased Blood Flow and Vascular Remodeling With Long-Term Ang-II Infusion

In a separate cohort, we tested the effects of longer-term Ang-II infusion over a 4-week period on retinal blood flow (Fig. 5A). The spontaneous systolic BP rose from 123 mm Hg at baseline to 162 mm Hg on days 14 and 28 (Fig. 5B). Within 6 weeks after the

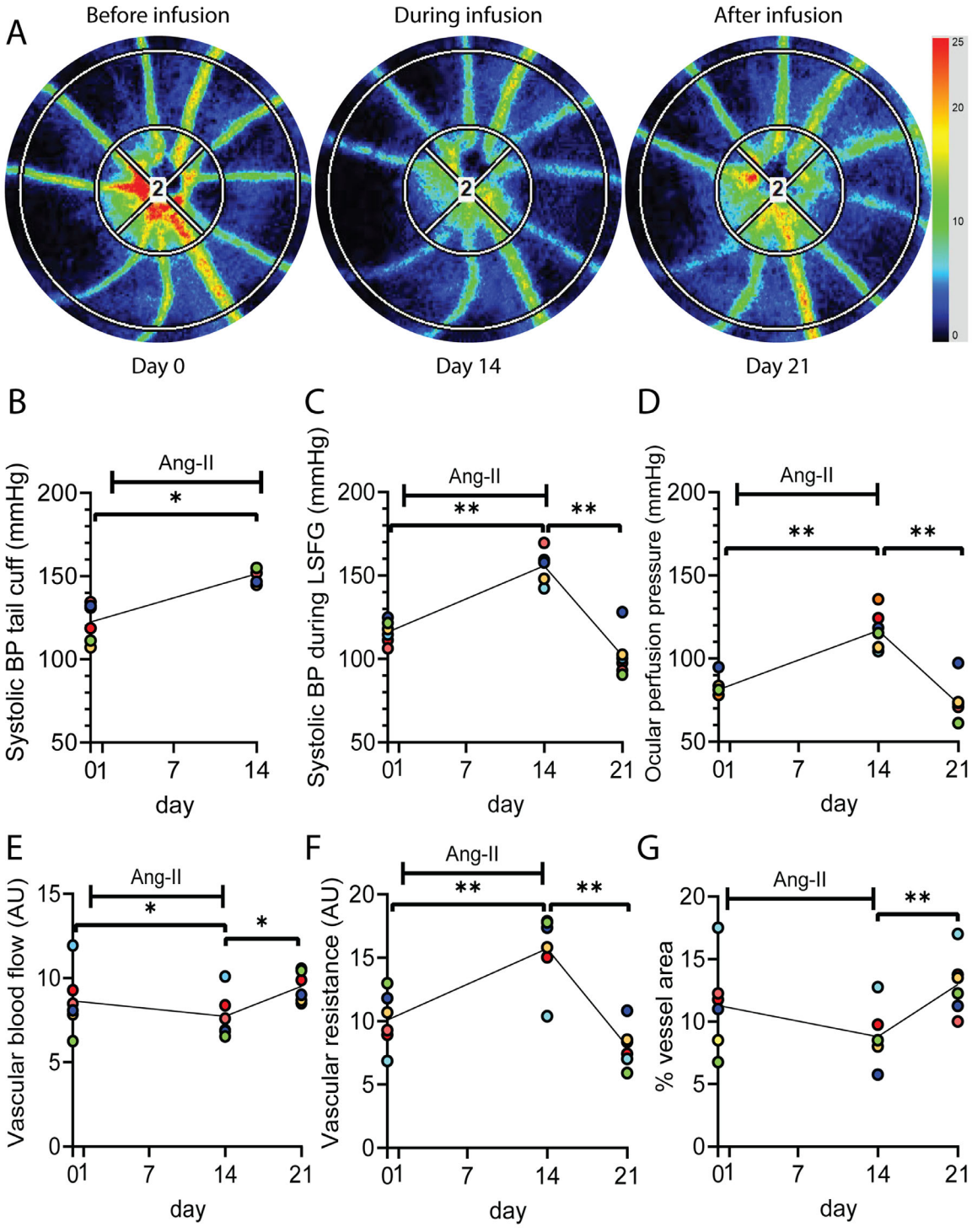

Figure 4. Regulation of retinal blood flow with infusion of Ang-II for 2 weeks. (**A**) Representative blood flow maps of a mouse imaged before infusion (*left*), during infusion (day 14, *center*), and 1 week after infusion was terminated (day 21, *right*). (**B**) Systolic BP (SBP) by tail cuff method and (**C**) during the LSFG imaging procedure in six male C57BL/6J mice. (**D**) Ocular perfusion pressure, (**E**) vascular blood flow (MV), (**F**) vascular resistance, and (**G**) percent vessel area at time points as indicated. $n = 6$, $^{*}P < 0.05$, $^{**}P < 0.01$ by Wilcoxon test in **B**, repeat measures 1-way ANOVA with Tukey's multiple comparisons test in **C** to **G**. Line indicates median values. Values from individual mice are color-coded.

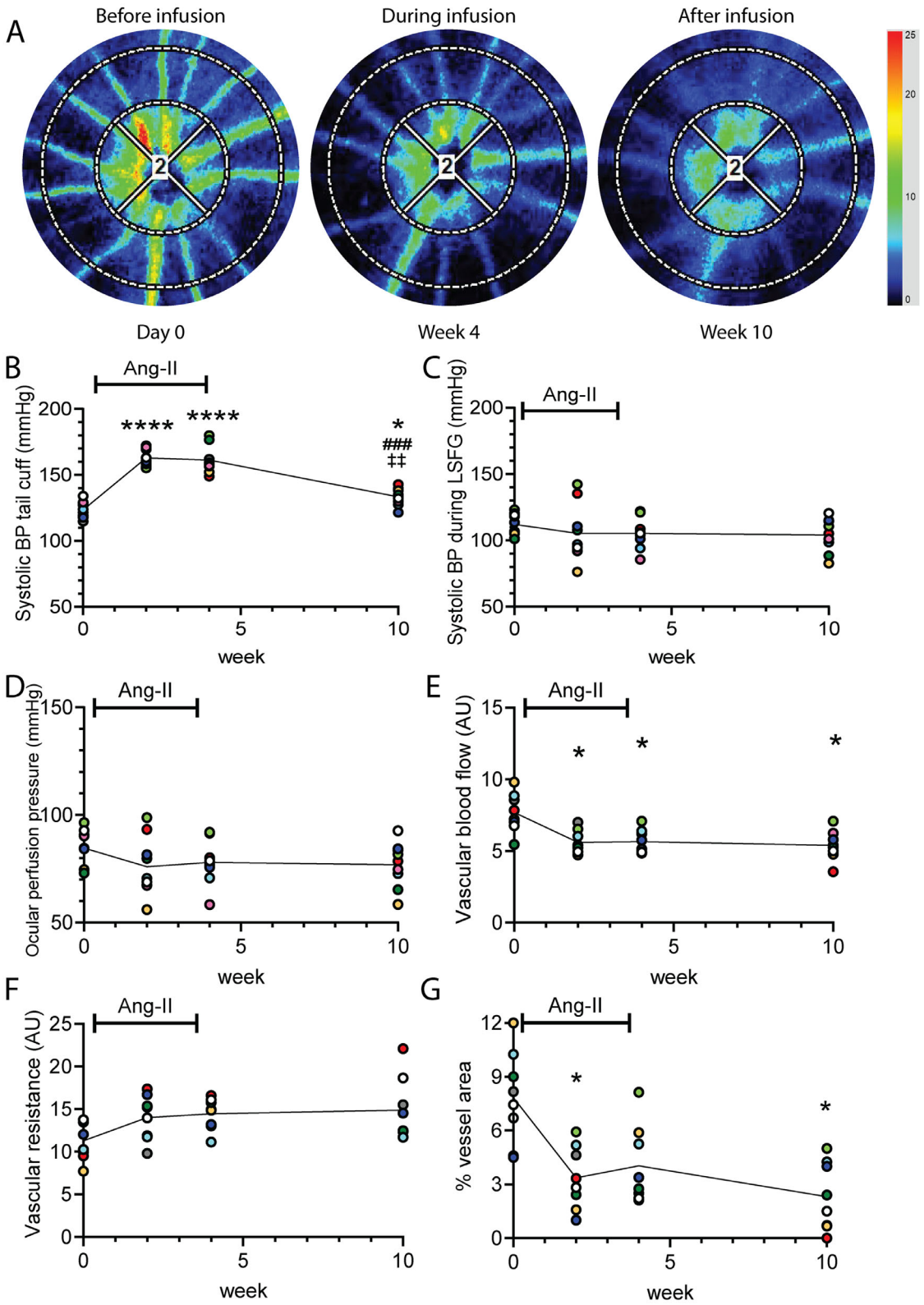

Figure 5. Chronic decreased blood flow and vascular remodeling with long-term Ang-II infusion. (**A**) Representative blood flow maps of a mouse imaged before infusion (*left*), during infusion (week 4, *center*), and 6 weeks after infusion was terminated (week 10, *right*). (**B**) Systolic BP (SBP) by tail cuff method and (**C**) during the LSFG imaging procedure in six male C57BL/6J mice. (**D**) Ocular perfusion pressure, (**E**) vascular blood flow (MV), (**F**) vascular resistance, and (**G**) percent vessel area at time points as indicated. $n = 8$, $^{*}P < 0.05$, $^{**}P < 0.01$, $^{***}P < 0.001$ compared to baseline, $^{\#\#\#}P < 0.001$ 2 weeks versus 10 weeks, $^{\ddagger\ddagger}P < 0.01$ 4 weeks versus 10 weeks, by repeat measures 1-way ANOVA with Holm-Sidak's multiple comparisons test. Line indicates median values. Values from individual mice are color-coded.

cessation of Ang-II infusion, systolic BP decreased significantly to 134 mm Hg, but remained elevated compared to baseline ($P < 0.05$). During the LSFG procedure, systolic BP (Fig. 5C) and OPP (Fig. 5D) were maintained at levels similar to those observed at baseline. Vascular blood flow decreased significantly by 2 weeks after the initiation of Ang-II infusion (from 7.7 AU at baseline to 5.6 AU) and remained low even after Ang-II infusion was terminated (5.4 AU at 10 weeks; Fig. 5E). Similarly, vascular resistance increased after 2 weeks (from 11.3 AU at baseline to 14.0 AU at 2 weeks), and remained elevated 6 weeks after Ang-II infusion was terminated (14.9 AU at 10 weeks; Fig. 5F) The percent vessel area decreased significantly after 2 weeks (from 7.8% at baseline to 3.4%) and did not recover within 6 weeks after Ang-II infusion was terminated (2.3% at 10 weeks; Fig. 5G).

Discussion

Here, we deployed LSFG to monitor retinal blood flow in normo- and hypertensive C57Bl/6 mice. First, we compared the analysis of blood flow parameters by an annular area of retina versus an individually defined retinal vessel analysis (TRAVA) method. In our hands, the less labor-intensive annular method yielded less variability between the scans and observers. Across 3 sessions, the coefficient of variability for vascular flow was 14.9%, well within the range previously reported in a rat model.[17] Moreover, blood flow was constant over a range of BPs, suggesting autoregulation of retinal blood flow as reported in humans.[22] Infusion of Ang-II for 2 weeks reduced blood flow with evidence for retinal vasoconstriction and increased vascular resistance. Within 1 week of termination of Ang-II administration, BP and blood flow parameters returned to those measured before Ang-II treatment. When Ang-II was administered for 4 weeks, evidence for reduced vascular blood flow, increased vascular resistance, and vasoconstriction persisted even at 6 weeks after Ang-II administration was terminated, suggesting that chronic changes in myogenic tone or structural remodeling had occurred. These data demonstrate that LSFG can detect changes in blood flow and vascular tone, as anticipated with Ang-II infusion, and that quantitative analysis of retinal blood flow by LSFG can be achieved in mice.

Although LSFG has been applied to study various ophthalmologic diseases in humans, reports on its use in rodent models, in particular with serial testing, have been limited. In a rat model of non-arteritic ischemic optic neuropathy after photoactivation of Rose Bengal dye, significant reductions in optic nerve head blood flow were detected over a study period of 28 days.[9] Serial measurements over the optic nerve head were also reported in Brown Norway rats over 60 weeks to determine age-dependent changes.[17] Moreover, constriction of retinal veins and decreased chorioretinal blood flow were observed after injection of endothelin-1 in nonpigmented spontaneously hypertensive rats, although no quantification was provided.[23]

In contrast, studies in mice are more limited in scope and analyses. LSFG has been used to compare baseline blood flow in three genetic models of diabetes.[18] Moreover, Nishinaka and colleagues demonstrated the efficacy of kallidinogenase, a serine proteinase that releases kinin, to improve blood flow in a retinal vein occlusion model by LSFG.[24] However, these studies did not analyze changes over time and, in comparison, to a baseline measurement in the same animal. Our study establishes that in mice, longitudinal measurements can be performed with low variability and reliably detect significant blood flow changes in a widely used model of hypertension by Ang-II infusion. Further, we introduce a surrogate readout for vasoconstriction by measuring vessel area above a fixed flow rate threshold. These findings indicate LSFG may be used to reliably assess longitudinal changes in response to pharmacological interventions.

The TRAVA method permits analysis of arterioles and venules separately, which is especially advantageous for studying localized, vessel-specific disorders, such as focal occlusion following branch retinal venous occlusion.[25] However, in our study, we were unable to reliably distinguish between retinal arterioles and venules in scanning light ophthalmoscopy (SLO) retinal images or in LSFG flow profiles in mice. In addition, analysis by TRAVA is more time-intensive, introduces variability based on how the operator defines the vessel boundaries, and requires the vascular blood flow to markedly exceed tissue flow. Conversely, the annulus method categorizes blood and tissue flow based on the histogram of pixelwise MBR across the annulus. It only requires the application of two concentric circular bands. Moreover, computation time, interoperator variability, and inter- and intrasession variabilities are lower than with the TRAVA method, making the annulus method preferable unless measurements in a single vessel are warranted. Of note, we found good agreement between the two methods (see Fig. 3).

Whereas Doppler OCT, an alternative quantitative method to measure blood flow, relies on the Doppler phenomenon, LSFG exploits the speckle phenomenon of laser light reflected from the fundus of the eye. Although recent progress has been made to overcome

the major limitation of Doppler angle-dependent velocities, the solutions require significant computational efforts or by multiple OCT detection beams and the instrumentation is currently not widely available, nor is it commercially available. In contrast, LSFG requires minimal time for recording and postprocessing and outputs dynamic measures of relative blood flow sampling all regions simultaneously. LSFG offers the advantage that equipment for imaging human subjects is FDA-approved and a very similar instrument for small animal research is also commercially available, making cross-translational studies feasible for a larger group of investigators. Data analysis is very similar for small animals and human subjects – it is straightforward, user-friendly, and requires comparably less computation time, meaning interoperator agreement is high (here, 0.928 for the annulus method). While offering lower resolution of microvascular structure, LSFG imaging can easily be adapted for flow measurements in single vessels or retinal or choroidal regions of interest. Of note, whereas Doppler OCT imaging has been reported to depict cerebral microvessel through the intact skull in mice, there are to our knowledge currently no reports on its use in the murine retina.

Because the retinal vasculature is morphologically and functionally related to the cerebral vessels, the noninvasive assessment of retinal vasculature provides an approach for cerebrovascular risk stratification in humans.[26,27] Here, we demonstrate that in mice, evidence for Ang-II-induced vasoconstriction of retinal vessels can be detected by LSFG. Surprisingly, 6 weeks after the end of Ang-II infusion, the vascular flow and the area in which a vascular flow signal was detected were still reduced (see Figs. 5E, G), providing evidence for chronic constriction or structural remodeling.

There are several limitations to the use of LSFG in mice. Although the analysis of single blood flow waveforms in humans holds the potential to provide additional valuable information regarding vascular stiffness and remodeling (e.g. in aging), dynamic analysis of blood flow changes during systole and diastole is hampered by higher physiologic heart rates in mice. An alternative approach that provides a power analysis of dynamics of blood flow as a function of frequency by Fourier analysis has been proposed and awaits further validation in animal models.[28] Moreover, the intensity of the LSFG signal originating from the choroid is limited largely by the level of pigment contained in the retinal pigment epithelium and choroid. In C57BL/6J mice, which have a darkly pigmented fundus, the deeper choroidal blood flow signal is not detected. The optimal mouse strain for imaging the choroidal circulation will need to be determined in further studies, with particular emphasis on adapting the imaging protocols. The use of various anesthesia protocols can differentially affect ocular blood flow.[29] In our study, we used ketamine and xylazine, which is associated with lower retinal blood flow compared to isoflurane. Regardless of anesthetic used, obtaining baseline measurements before interventions provides a suitable reference. Another limitation of this study is that it cannot be conclusively determined whether the persistent reductions in retinal blood flow after chronic Ang-II infusion are due to chronic changes in myogenic tone or to structural remodeling of the vessel wall. Coupling LSFG imaging with other assessments of oxygenation by phosphorescence lifetime imaging may provide greater understanding into tissue perfusion in hypertension.

Acknowledgments

Supported by the American Heart Association (18IPA34170003 to I.M.G.; 20PRE35110054 to M.R.T.), the National Institutes of Health (R01 EY031544 to I.M.G. and R.H.K.; T32 CA078586 to M.R.T.), and the US Department of Veterans Affairs (I01BX000163 to I.M.G. and I50RX003002 to R.H.K.).

Disclosure: **M.R. Tamplin**, None; **K.A. Broadhurst**, None; **A.H. Vitale**, None; **R. Hashimoto,** None; **R.H. Kardon**, None; **I.M. Grumbach**, None

References

1. Townsend-Pico WA, Meyers SM, Lewis H. Indocyanine green angiography in the diagnosis of retinal arterial macroaneurysms associated with submacular and preretinal hemorrhages: a case series. *Am J Ophthalmol.* 2000;129(1):33–37.
2. Patwardhan RV, Smith OJ, Farmelant MH. Serum transaminase levels and cholescintigraphic abnormalities in acute biliary tract obstruction. *Arch Intern Med.* 1987;147(7):1249–1253.
3. Liu W, Yi J, Chen S, Jiao S, Zhang HF. Measuring retinal blood flow in rats using Doppler optical coherence tomography without knowing eyeball axial length. *Med Phys.* 2015;42(9):5356–5362.
4. Konishi N, Fujii H. Real-time visualization of retinal microcirculation by laser flowgraphy. *Optical Eng.* 1995;34(3):753–757.
5. Wang L, Cull GA, Piper C, Burgoyne CF, Fortune B. Anterior and posterior optic nerve head blood flow in nonhuman primate experimental glaucoma

model measured by laser speckle imaging technique and microsphere method. *Invest Ophthalmol Vis Sci.* 2012;53(13):8303–8309.
6. Witkowska KJ, Bata AM, Calzetti G, et al. Optic nerve head and retinal blood flow regulation during isometric exercise as assessed with laser speckle flowgraphy. *PLoS One.* 2017;12(9):e0184772.
7. Sato T, Sugawara J, Aizawa N, et al. Longitudinal changes of ocular blood flow using laser speckle flowgraphy during normal pregnancy. *PLoS One.* 2017;12(3):e0173127.
8. Fondi K, Bata AM, Luft N, et al. Evaluation of flicker induced hyperemia in the retina and optic nerve head measured by laser speckle flowgraphy. *PLoS One.* 2018;13(11):e0207525.
9. Takako H, Hideki C, Nobuhisa NI. Evaluation of optic nerve head blood flow in normal rats and a rodent model of non-arteritic ischemic optic neuropathy using laser speckle flowgraphy. *Graefes Arch Clin Exp Ophthalmol.* 2017;255(10):1973–1980.
10. Aizawa N, Yokoyama Y, Chiba N, et al. Reproducibility of retinal circulation measurements obtained using laser speckle flowgraphy-NAVI in patients with glaucoma. *Clin Ophthalmol.* 2011;5:1171–1176.
11. Enaida H, Okamoto K, Fujii H, Ishibashi T. LSFG findings of proliferative diabetic retinopathy after intravitreal injection of bevacizumab. *Ophthalmic Surg Lasers Imaging.* 2010;41(Online):e1–e3.
12. Arimura T, Shiba T, Takahashi M, et al. Assessment of ocular microcirculation in patients with end-stage kidney disease. *Graefes Arch Clin Exp Ophthalmol.* 2018;256(12):2335–2340.
13. Shiba T, Takahashi M, Matsumoto T, Shirai K, Hori Y. Arterial stiffness shown by the cardio-ankle vascular index is an important contributor to optic nerve head microcirculation. *Graefes Arch Clin Exp Ophthalmol.* 2017;255(1):99–105.
14. Hayashi H, Okamoto M, Kawanishi H, et al. Association between optic nerve head blood flow measured using laser speckle flowgraphy and radial arterial pressure during aortic arch surgery. *J Cardiothorac Vasc Anesth.* 2018;32(2):702–708.
15. Hayashi H, Okamoto M, Kawanishi H, et al. Ocular blood flow measured using laser speckle flowgraphy during aortic arch surgery with antegrade selective cerebral perfusion. *J Cardiothorac Vasc Anesth.* 2016;30(3):613–618.
16. Ritt M, Harazny JM, Ott C, et al. Impaired increase of retinal capillary blood flow to flicker light exposure in arterial hypertension. *Hypertension.* 2012;60(3):871–876.
17. Wada Y, Higashide T, Nagata A, Sugiyama K. Longitudinal changes in optic nerve head blood flow in normal rats evaluated by laser speckle flowgraphy. *Invest Ophthalmol Vis Sci.* 2016;57(13):5568–5575.
18. Chaurasia SS, Lim RR, Parikh BH, et al. The NLRP3 inflammasome may contribute to pathologic neovascularization in the advanced stages of diabetic retinopathy. *Sci Rep.* 2018;8(1):2847.
19. Remer I, Pierre-Destine LF, Tay D, Golightly LM, Bilenca A. In vivo noninvasive visualization of retinal perfusion dysfunction in murine cerebral malaria by camera-phone laser speckle imaging. *J Biophotonics.* 2019;12(1):e201800098.
20. Longo A, Geiser MH, Riva CE. Posture changes and subfoveal choroidal blood flow. *Invest Ophthalmol Vis Sci.* 2004;45(2):546–551.
21. Shrout PE, Fleiss JL. Intraclass correlations: uses in assessing rater reliability. *Psychol Bull.* 1979;86(2):420–428.
22. Robinson F, Riva CE, Grunwald JE, Petrig BL, Sinclair SH. Retinal blood flow autoregulation in response to an acute increase in blood pressure. *Invest Ophthalmol Vis Sci.* 1986;27(5):722–726.
23. Kida T, Flammer J, Oku H, et al. Vasoactivity of retinal veins: a potential involvement of endothelin-1 (ET-1) in the pathogenesis of retinal vein occlusion (RVO). *Exp Eye Res.* 2018;176:207–209.
24. Nishinaka A, Fuma S, Inoue Y, Shimazawa M, Hara H. Effects of kallidinogenase on retinal edema and size of non-perfused areas in mice with retinal vein occlusion. *J Pharmacol Sci.* 2017;134(2):86–92.
25. Fukami M, Iwase T, Yamamoto K, Kaneko H, Yasuda S, Terasaki H. Changes in retinal microcirculation after intravitreal ranibizumab injection in eyes with macular edema secondary to branch retinal vein occlusion. *Invest Ophthalmol Vis Sci.* 2017;58(2):1246–1255.
26. Lehmann MV, Schmieder RE. Remodeling of retinal small arteries in hypertension. *Am J Hypertens.* 2011;24(12):1267–1273.
27. Cheung CY, Ikram MK, Sabanayagam C, Wong TY. Retinal microvasculature as a model to study the manifestations of hypertension. *Hypertension.* 2012;60(5):1094–1103.
28. Kikuchi S, Miyake K, Tada Y, et al. Laser speckle flowgraphy can also be used to show dynamic changes in the blood flow of the skin of the foot after surgical revascularization. *Vascular.* 2019;27(3):242–251.
29. Moult EM, Choi W, Boas DA, et al. Evaluating anesthetic protocols for functional blood flow imaging in the rat eye. *J Biomed Opt.* 2017;22(1):16005.